Solar Energy Materials & Solar Cells 230 (2021) 111198

Contents lists available at ScienceDirect

Solar Energy Materials and Solar Cells

journal homepage: www.elsevier.com/locate/solmat

Radiative recombination in silicon photovoltaics: Modeling the influence of charge carrier densities and photon recycling

Andreas Fell [a,*], Tim Niewelt [a,b], Bernd Steinhauser [a], Friedemann D. Heinz [a,b], Martin C. Schubert [a], Stefan W. Glunz [a,b]

[a] Fraunhofer Institute for Solar Energy Systems (ISE), Heidenhofstrasse 2, 79110, Freiburg, Germany
[b] Department of Sustainable Systems Engineering (INATECH), Albert Ludwig University of Freiburg, Emmy-Noether-Str. 2, D-79110, Freiburg, Germany

ARTICLE INFO

Keywords:
Radiative recombination
B_{rel}
Silicon
Photon recycling
Free carrier absorption
Band gap narrowing

ABSTRACT

In order to push silicon solar cell efficiencies further towards their limit, as well as to ensure accuracy of luminescence based characterization techniques, an accurate modeling of radiative recombination is important. It is well-known that the radiative recombination coefficient B_{rad} of silicon shows a substantial charge carrier density dependence (c-dependence), often modelled via the scaling factor B_{rel} quantified by Altermatt et al. Another effect lowering the total radiative recombination is photon recycling (PR), which depends mainly on the width and optical properties of the sample. PR also depends on free-carrier absorption (FCA), which introduces a further c-dependence. This work comprehensively reassesses and quantifies those influences on radiative recombination in silicon for photovoltaic (PV) applications. Firstly, it is evidenced that Altermatt's B_{rel} model is dominated by the effect of band-gap narrowing (BGN). This clarifies that it should not be combined with a different BGN model to avoid modeling inconsistencies. It is thereby further confirmed that the band-to-band absorption coefficient of silicon does not show a relevant c-dependence for PV conditions. Next, a PR model is suggested which calculates a scaling factor $B_{rel,PR}$. The model is proven useful in improving the interpretation of very high lifetime measurements. Finally, it is found that the c-dependence introduced by FCA affects the direct proportionality between luminescence signal and radiative recombination beyond charge carrier densities of 10^{16} cm^{-3} for samples thicker than typical wafer widths, and should then be considered in characterization techniques like e.g. calibrated lifetime measurements via photoluminescence.

1. Introduction

While radiative recombination plays a minor role for the performance of a practical silicon solar cell, it's of great importance for fundamental modeling and for electro-optical characterization of silicon solar cells and wafers. The radiation escaping the sample is the fundamental measurement quantity of all luminescence-based characterization techniques, which have become highly popular in the silicon PV community. Furthermore, on the push to record solar cell conversion efficiencies, material and surface passivation quality are now able to reach such levels which result in radiative recombination to observably limit the measured effective lifetime. In order to ensure accuracy of luminescence-based measurements, as well as to properly interpret recombination losses in very-high-lifetime samples, an accurate quantification of radiative recombination is thus important, and will be reviewed and reassessed in this work for the case of silicon.

Modeling of radiative recombination is most commonly done using a bimolecular recombination coefficient, i.e. the radiative recombination coefficient B_{rad}, which is defined as the proportionality factor between the product of hole and electron density pn and the radiative recombination rate R_{rad} [1]:

$$R_{rad} = B_{rad} pn. \tag{1}$$

An alternative modeling approach is the fundamental thermodynamic relationship between R_{rad} and the separation of the quasi-Fermi energies $\Delta\eta$ first described by Kennard [2] and later by Ross [3], which became popular as the generalized Planck law by Würfel et al. [4], who extended the theory to indirect transitions:

$$R_{rad} = \int_0^\infty r_{spont}(\hbar\omega, \Delta\eta) d(\hbar\omega) = \frac{1}{\pi^2 \hbar^3 c_0^2} \int_0^\infty \frac{(\hbar\omega)^2 n^2 \alpha_{bb}}{\exp\left(\frac{\hbar\omega - \Delta\eta}{kT}\right) - 1} d(\hbar\omega) \tag{2}$$

* Corresponding author.
E-mail address: andreas.fell@ise.fraunhofer.de (A. Fell).

https://doi.org/10.1016/j.solmat.2021.111198
Received 18 February 2021; Received in revised form 17 May 2021; Accepted 22 May 2021
Available online 2 June 2021

Here $r_{spont}(\hbar\omega, \Delta\eta)$ denotes the spontaneous emission rate per photon energy $\hbar\omega$, n the real part of the refractive index, α_{bb} the band-to-band absorption coefficient, c_0 the speed of light, T the temperature and k the Boltzmann constant. Assuming a non-degenerate semiconductor, the minus one in the denominator can be neglected, and the Boltzmann approximation $pn = n_{i,eff}^2 \exp\left(\frac{\Delta\eta}{kT}\right)$ can be used to calculate B_{rad} from equations (1) and (2) [5]:

$$B_{rad} = \frac{1}{n_{i,eff}^2} \frac{1}{\pi^2 \hbar^3 c_0^2} \int_0^\infty \frac{(\hbar\omega)^2 n^2 \alpha_{bb}}{\exp\left(\frac{\hbar\omega}{kT}\right)} d(\hbar\omega), \tag{3}$$

where $n_{i,eff}$ denotes the effective intrinsic carrier density.

As noted in Ref. [5], equations (1) and (3) reveal two ways B_{rad} can be determined. Either by measuring both the charge carrier densities and the absolute luminescence signal and using equation (1), as in Refs. [1,6] for silicon or, as demonstrated in more recent works for silicon, instead by using spectrally resolved values for n and α_{bb} along with modeling $n_{i,eff}$ and apply equation (3), as in Refs. [5,7].

It is well known that B_{rad} is not strictly constant, but may show a substantial dependence on charge carrier density (c-dependence) either via doping or via electro-optical carrier injection. For silicon, the c-dependence of B_{rad} is most commonly modelled via a scaling factor B_{rel} applied to a low carrier density limit $B_{rad,low}$, which was parameterized by Altermatt et al. [8]. Equation (3) allows factoring B_{rel} into an electrical and optical part:

$$B_{rad} = B_{rad,low} B_{rel,el} B_{rel,opt} \tag{4}$$

The electrical part $B_{rel,el}$ quantifies the c-dependence of $n_{i,eff}$ via band-gap narrowing (BGN), and the optical part $B_{rel,opt}$ quantifies the c-dependence of the spectral absorption coefficient α_{bb} and refractive index n.

Another well-known effect influencing the effective radiative recombination rate is photon recycling (PR). Photons emitted via radiative recombination are partly contributing to generation rate via band-to-band absorption, effectively lowering the radiative recombination rate. In contrast to $B_{rel,el}$ and $B_{rel,opt}$, PR does not change the rate of radiative emission, but the compensating generation via reabsorption within a macroscopic sample can be interpreted as a reduced net recombination rate. PR is dependent on the sample's width and optical properties, which determine the probability of band-to-band reabsorption $f_{reabs,bb}$. If $f_{reabs,bb}$ is known, a simple approach to account for PR is to apply another scaling factor $B_{rel,PR} = 1 - f_{reabs,bb}$ to equation (1):

$$R_{rad,eff} = B_{rad} B_{rel,PR} pn = B_{rad}\left(1 - f_{reabs,bb}\right) pn \tag{5}$$

A usually neglected effect is the c-dependence of PR via free carrier absorption (FCA) [9]. As increasing charge carrier densities increase FCA, the band-to-band reabsorption becomes less efficient, which lowers $f_{reabs,bb}$ and thereby increases the net radiative recombination rate.

Starting with reviewing the value for $B_{rad,low}$, this work comprehensively discusses each influencing factor of B_{rad}, and suggests best-practices modeling approaches. To model the PR effect, an approach similar to Refs. [10,11] is proposed, via extending an existing light-trapping model to predict $f_{reabs,bb}$. Finally, the model is used to theoretically predict the c-dependence of PR and luminescence intensity.

2. The low carrier density limit

The radiative recombination coefficient at low carrier densities, i.e. at intrinsic conditions, is best quantified by the product $B_{rad,low} n_{i,0}^2$:

$$B_{rad,low} n_{i,0}^2 = \frac{1}{\pi^2 \hbar^3 c_0^2} \int_0^\infty \frac{(\hbar\omega)^2 n^2 \alpha_{bb}}{\exp\left(\frac{\hbar\omega}{kT}\right)} d(\hbar\omega), \tag{6}$$

as this definition does not require a value for n_i but is solely a function of the material's intrinsic optical properties. As will be shown in the next section, this quantity in fact does not show any observable c-dependence for silicon for typical photovoltaic operating conditions, and is thus considered a more fundamental property compared to $B_{rad,low}$ alone.

The latest work on determining $B_{rad,low}$ as a function of temperature by Nguyen et al. [7] in fact already provided a parameterization of $B_{rad,low} n_{i,0}^2$ via their equation (3), with T in K and $B_{rad,low} n_{i,0}^2$ in $cm^{-3}s^{-1}$:

$$log_{10}\left(B_{rad,low} n_{i,0}^2\right) = -176.98 + 2.68812 \times T - 0.018137 \times T^2 + 6.56769 \times 10^{-5} \times T^3 - 1.21382 \times 10^{-7} \times T^4 + 8.99086 \times 10^{-11} \times T^5. \tag{7}$$

$B_{rad,low} n_{i,0}^2$ can also be calculated from the most recent optical properties of silicon published by Schinke et al. [12] via equation (6). Those two options are compared in Fig. 1, showing overall close agreement. The deviations are in the range of 10%, which is consistent with the uncertainty given by Schinke et al. At 300 K, $B_{rad,low} n_{i,0}^2$ equals $4.853 \times 10^5 cm^{-3} s^1$ for Nguyen et al. and $4.535 \times 10^5 cm^{-3} s^1$ for Schinke et al., respectively.

For convenience of the reader, the latest models to quantify $n_{i,0}$ as a function of temperature are given in the following. The BGN-free intrinsic charge carrier density $n_{i,0}$ was most recently parameterized by Couderc et al. [13], which is consistent with the latest value of $9.65 \times 10^9 cm^{-3}$ at 300 K determined by Altermatt et al. [14]:

$$n_{i,0} = 1.541 \times 10^{15} T^{1.712} exp\left(-\frac{E_g^0}{2kT}\right), \tag{8}$$

with the temperature dependence of the intrinsic band-gap E_g^0 given by Pässler [15]:

$$E_g^0 = 1.17eV - 0.1441eV \left[\frac{1 - 3\Delta^2}{exp\left(\frac{2}{\chi}\right) - 1} + \frac{3\Delta^2}{2}\left(1 + \frac{\pi^2}{3(1+\Delta^2)}\chi^2 + \frac{3\Delta^2 - 1}{4}\chi^3 + \frac{8}{3}\chi^4 + \chi^6\right)^{\frac{1}{6}} - 1\right], \tag{9}$$

with $\chi = \frac{2T}{446K}$ and $\Delta = 0.51$.

3. Influence of band-gap-narrowing

This section reassesses the c-dependence of B_{rad} introduced by BGN for silicon for typical photovoltaic conditions. The band-gap reduction $\Delta E_{g,BGN}$ impacts the electrical part $B_{rel,el}$ by

$$B_{rel,el} = \frac{n_{i,0}^2}{n_{i,eff}^2} = exp\left(-\frac{\Delta E_{g,BGN}}{kT}\right), \tag{10}$$

which can be calculated by the well-established theoretical BGN model

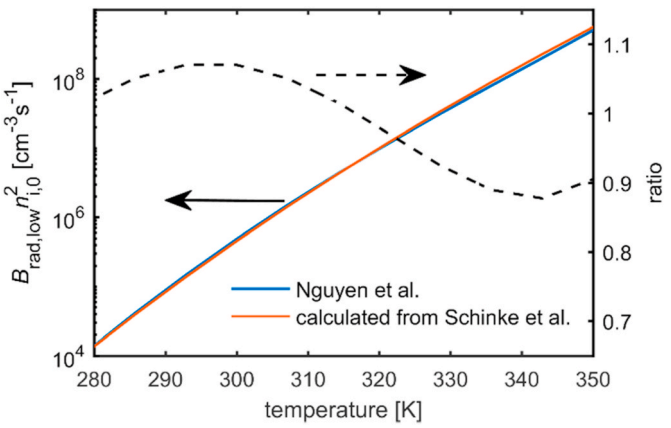

Fig. 1. Comparison of $B_{rad,low} n_{i,0}^2$ of silicon as given by Nguyen et al. [7] with the one calculated from the data of Schinke et al. [12] using equation (6), together with their ratio, for relevant photovoltaic device operating temperatures.

of Schenk [16]. $\frac{n_{i,0}^2}{n_{i,eff}^2}$ is plotted together with the semi-empirical B_{rel} model by Altermatt et al. [8] as well as the underlying experimental data of Schlangenotto et al. [6] in Fig. 2 and Fig. 3, for the injection-dependence and doping-dependence, respectively. It can be seen that Schenk's BGN model alone explains the experimental data equally well as Altermatt's B_{rel} model, which leads to the following conclusions:

i) The c-dependence of B_{rad} is largely dominated by the effect of BGN on n_i, i.e. $B_{rel} \cong B_{rel,el}$;
ii) the c-dependence of the optical properties of silicon, most notably of the absorption coefficient α_{bb}, has a much smaller effect on B_{rel} and is not quantifiable from the presented data, meaning that $B_{rel,opt} \cong 1$ is the only sensible assumption for the investigated range of charge carrier densities;
iii) Altermatt's B_{rel} model consequently must be interpreted as a parameterization of BGN;
iv) it follows that the quantity $B_{rad,low} n_{i,0}^2$ does not show a significant c-dependence.

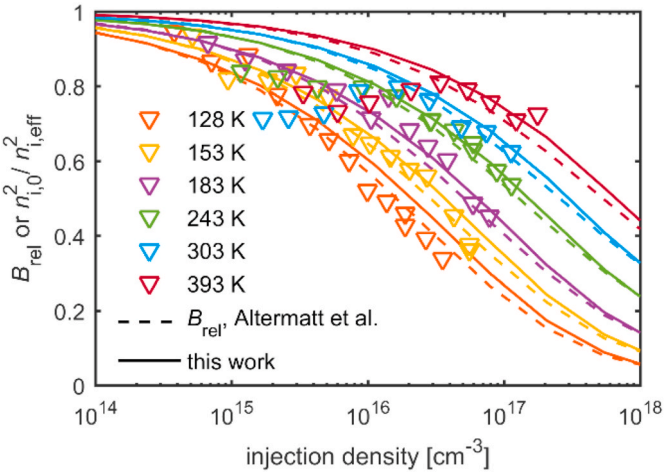

Fig. 2. Injection dependence of B_{rel}; comparison of the experimental data of Schlangenotto et al. [6] (as normalized in Ref. [8]) with the B_{rel} model of Altermatt et al. [8] and with this work's calculations using Schenk's BGN model [16].

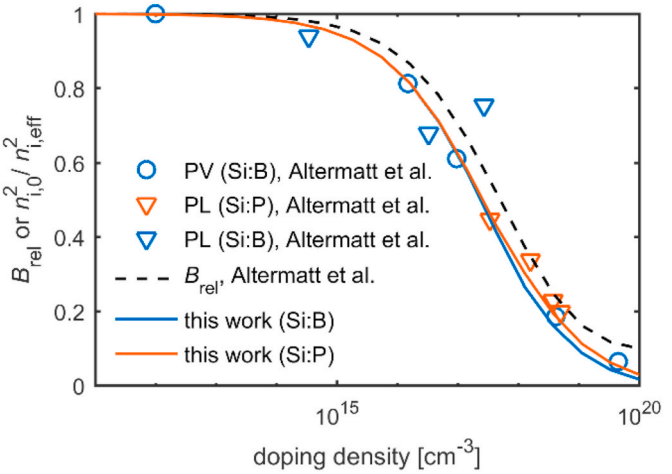

Fig. 3. Doping density dependence of B_{rel}; comparison of the experimental data of Altermatt et al. [8] with their B_{rel} model and with this work's calculations using Schenk's BGN model [16].

This confirms an assumption almost exclusively applied to date in silicon solar cell modeling: the band-to-band absorption coefficient does not change significantly with charge carrier density. Note that fundamentally a change of α_{bb} is expected in particular towards very high charger carrier densities like e.g. in lasing applications. A measurement for charge carrier densities relevant for PV was presented in Ref. [17]. However, the main influence was observed for wavelengths well above the band-gap not affecting PV applications, while for near-band-gap wavelengths the effect is small and possibly within the measurement inaccuracy. So for now, assuming α_{bb} as c-independent appears to be the only appropriate assumption for silicon solar cell modeling.

The fact that Altermatt's B_{rel} model represents a BGN model means that it should not be mixed with Schenk's BGN model. However, Schenk's BGN model is mathematically rather complex, so if an implementation is not easily accessible, Altermatt's B_{rel} model can be used as a simpler alternative BGN model in applications also other than radiative recombination. Notably, it includes temperature dependence in contrast to other simple BGN models [18,19].

The invariability of $B_{rad,low}n_{i,0}^2$ further confirms the validity of the strict direct proportionality between radiative recombination rate and Fermi-level splitting:

$$R_{rad} = B_{rad,low}n_{i,0}^2 \exp\left(\frac{\Delta\eta}{kT}\right). \tag{11}$$

Equation (11) thus provides a simplistic but accurate way to model radiative recombination when the Fermi-level splitting instead of carrier densities are known, e.g. within solar cell modeling or from a voltage measurement, without the need for any B_{rel}, BGN or n_i model.

4. Photon reabsorption and photon escape

The escape probability of radiatively emitted photons determines the measurable luminescence signal of the sample, and the band-to-band part of the reabsorption leads to photon recycling. Both effects depend not only on the optical material properties, but also on the specific sample's width W and optical surface properties. Here an extension of the analytical light-trapping model by Basore [20] is used to model both effects, with variants thereof already presented to calculate escape probability [21]. The extension presented here derives a formula for $f_{reabs,bb}$ with a similar approach as in Refs. [10,11], and adds the impact of FCA on both f_{esc} of $f_{reabs,bb}$.

4.1. Analytical light trapping and photon escape model - review

The main inputs into the model which calculates light-trapping for external illumination are the first pass and nth pass internal reflections on the front and back side, R_{f1}, R_{fn}, R_{b1} and R_{bn}, respectively. Additionally, one needs to define the transmission of external illumination through the front surface layers T_{ext}, the facet angle representative for the front surface texture (zero for planar), and whether each surface reflects the light fully specular or fully diffusive. Main outputs of the model are the reflectance R, absorptance A and transmittance T (RAT), where the total reflectance R is separated into external reflectance and escape reflectance $R = R_{ext} + R_{esc}$. An overview of the model is sketched in Fig. 4.

The escape probability f_{esc} as a function of wavelength λ and position z can be derived from the light-trapping model via the reciprocity of emission and absorption [21]:

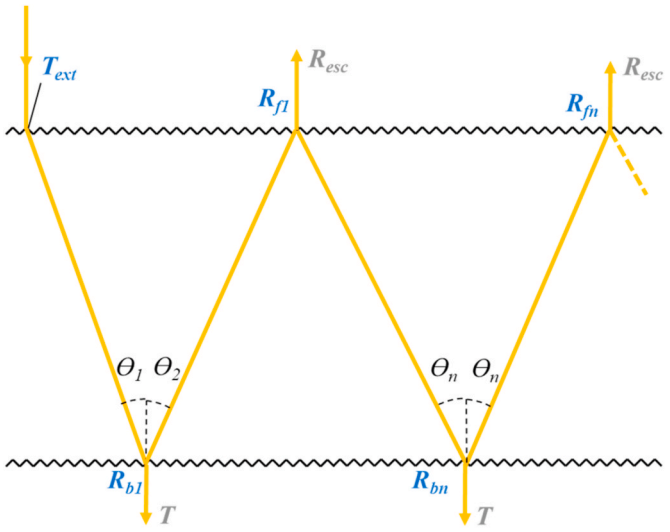

Fig. 4. Sketch of the light-trapping model used in this work as presented in Ref. [20], showing the first, second and subsequent nth passes of a representative illumination light ray through the sample.

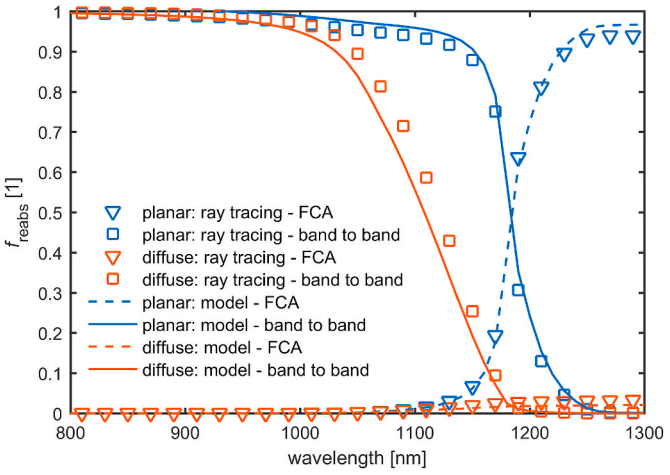

Fig. 5. Wavelength dependence of the photon reabsorption probability for a 150 μm thick bare silicon sample with an acceptor doping density of 10^{16} cm^{-3}, comparing ray-tracing results (*symbols*) with this work's analytical model (*lines*) for a *planar* sample and a sample with idealized Lambertian surfaces (*diffuse*).

with Ω being the acceptance angle of the detection optics, which is assumed to be small for the reciprocity, and $\alpha = \alpha_{bb} + \alpha_{FCA}$ being the total absorption coefficient from band-to-band and free carrier absorption.

Here θ_1, θ_2 and θ_n are the first, second and nth pass angle of an incident light ray, which are related to the respective transmission T_1, T_2 and T_n via

$$T_{i=1,2,n} = e^{\frac{-\alpha W}{\cos\theta_i}} \tag{13}$$

θ_1 is determined using Snell's law and a facet angle representing the surface texture, θ_2 and θ_n take on the same value after reflection from a specular surface. In case any side is defined to be diffusive, T_n, and

$$f_{esc}(\lambda, z) = \frac{\Omega}{4\pi n^2} T_{ext}\left[\frac{1}{\cos\Theta_1} e^{\frac{-\alpha z}{\cos\theta_1}} + \frac{T_1 R_{b1}}{\cos\theta_2} e^{\frac{-\alpha(W-z)}{\cos\theta_2}} + \frac{T_1 R_{b1} T_2 R_{f1}}{(1 - T_n^2 R_{bn} R_{fn})\cos\theta_n}\left(e^{\frac{-\alpha z}{\cos\theta_n}} + T_n R_{bn} e^{\frac{-\alpha(W-z)}{\cos\theta_2}}\right)\right], \tag{12}$$

subsequently θ_n, is determined by assuming a Lambertian angular distribution resulting in [22].

$$T_n = e^{-\alpha W}(1-\alpha W) - (\alpha W)^2 Ei(-\alpha W), \tag{14}$$

with $Ei(x)$ being the exponential integral function. θ_2 and T_2 take the same values if the rear side is diffusive.

4.2. Photon reabsorption model extension

The reabsorption probability $f_{\mathrm{reabs}}(\lambda,\theta,z)$ of a ray emitted at a depth z with an angle θ with unity intensity is calculated as follows: on the first pass to the surface the transmission is $e^{\frac{-\alpha z}{\cos\theta}}$, and the absorption $1-e^{\frac{-\alpha z}{\cos\theta}}$. For all subsequent passes the intensity is then lowered by the average reflection at the front and back side $R(\theta)=\frac{R_b(\theta)+R_f(\theta)}{2}$ and by the transmission through the wafer $T(\theta)=e^{\frac{-\alpha W}{\cos\theta}}$. This results in the geometric sum

$$\begin{aligned} f_{\mathrm{reabs}}(\lambda,\theta,z) &= 1-e^{\frac{-\alpha z}{\cos\theta}} + e^{\frac{-\alpha z}{\cos\theta}} R(\theta)(1-T(\theta))\left[1+R(\theta)T(\theta)\right. \\ &\left. + (R(\theta)T(\theta))^2 + \ldots\right] = 1-e^{\frac{-\alpha z}{\cos\theta}}\left(\frac{R(\theta)(1-T(\theta))}{1-R(\theta)T(\theta)}-1\right). \end{aligned} \tag{15}$$

Integration over the width for uniform emission throughout the sample width then yields

$$f_{\mathrm{reabs}}(\lambda,\theta) = \frac{1}{W}\int_0^W f_{\mathrm{reabs}}(\lambda,\theta,z)dz = 1-\frac{1-T(\theta)}{\frac{\alpha W}{\cos\theta}}\left(1-\frac{R(\theta)(1-T(\theta))}{1-R(\theta)T(\theta)}\right). \tag{16}$$

Next, a *diffuse* case is considered. The diffuse case reasonably represents samples with at least one scattering surface, where the combination with the isotropic radiative emission results in a randomized angular distribution for all passes. f_{reabs} can then be approximately calculated by the single average angle θ_n and transmission T_n as for the light-trapping model to

$$f_{\mathrm{reabs,diffuse}}(\lambda) = 1-\frac{1-T_n}{\frac{\alpha W}{\cos\theta_n}}\left(1-\frac{(1-T_n)\frac{R_{bn}+R_{fn}}{2}}{1-T_n\frac{R_{bn}+R_{fn}}{2}}\right). \tag{17}$$

In a second *planar* case, a planar interface to air is assumed on both sides. Due to total internal reflection and reabsorption, this case leads to a significant change of the angular distribution for subsequent passes. This invalidates the use of a representative transmission angle for all passes, and thus requires to integrate the angular reabsorption for isotropic angular emission represented by a $\sin\theta$ distribution:

$$f_{\mathrm{reabs,planar}}(\lambda) = \int_0^{\frac{\pi}{2}}\left[1-\frac{1-T(\theta)}{\frac{\alpha W}{\cos\theta}}\left(1-\frac{(1-T(\theta))R(\theta)}{1-T(\theta)R(\theta)}\right)\right]\sin\theta d\theta. \tag{18}$$

For the validation, Monte-Carlo ray-tracing simulations are performed using a self-coded implementation in Matlab®, equivalent to Ref. [23]. For each wavelength, rays are started with a random origin and direction within the sample representing isotropic spontaneous emission. For the case of a planar surface, rays are reflected with $R(\theta)$ calculated via the Fresnel equations. For a Lambertian surface, $R(\theta)$ is still calculated using the Fresnel equations, but the reflected direction is randomized following a cosine distribution. This approximates an ideal Lambertian surface, for which the internal reflections in the analytical model are set to the Lambertian limit [22]: $R_f = R_b = 1-\frac{1}{n^2}$. The ray-tracing and analytical model results are compared in Fig. 5 for a 150 µm thick bare silicon sample at 300 K with an acceptor doping density of 10^{16} cm^{-3}, using α_{bb} and refractive index data of Schinke et al. [12], and α_{FCA} of Baker-Finch et al. [24]. It can be seen that reabsorption at weakly absorbing wavelengths is much more effective in a planar sample, as also found in Ref. [23]. This is due to total internal reflections: without any scattering, all rays with an initial angle greater than the critical angle must be fully reabsorbed. The proportion of those angles is independent of the sample width, explaining why reabsorption stays high towards thinner samples, see Fig. 6.

The visible deviation between the model and the ray-tracer for the diffuse case is related to differences in the internal reflection: the ideal Lambertian limit of $1-\frac{1}{n^2}$ effectively assumes zero reflection for angles smaller than the critical angle. The deviations can be almost entirely removed when using a more elaborate expression [22] for better consistency with the ray-tracing. However, it is unclear which value best represents real scattering surfaces, therefore we stick to the simpler and well established ideal Lambertian limit.

Assuming uniform charge carrier densities, the total band-to-band reabsorption probability $f_{\mathrm{reabs,bb}}$ can be calculated by weighting with the spontaneous emission rate and the band-to-band fraction of the absorption coefficient:

$$f_{\mathrm{reabs,bb}} = \frac{\int f_{\mathrm{reabs}}(\lambda)\frac{\alpha_{\mathrm{bb}}}{\alpha_{\mathrm{bb}}+\alpha_{\mathrm{FCA}}} r_{\mathrm{spont}}(\lambda)d\lambda}{\int r_{\mathrm{spont}}(\lambda)d\lambda} \tag{19}$$

Equivalently, a single quantity for the escape probability can be

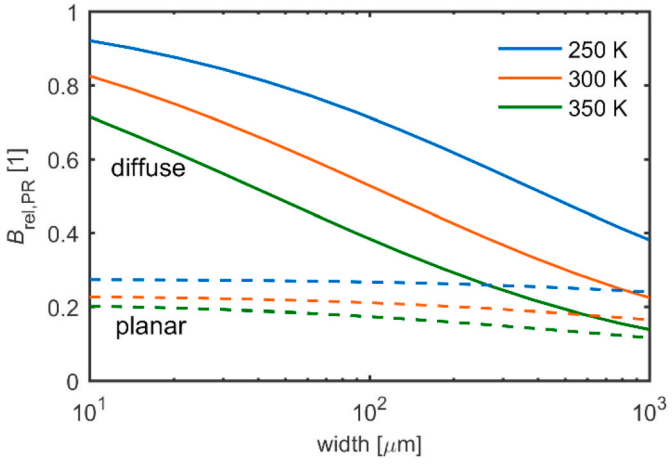

Fig. 6. Magnitude of the photon recycling effect quantified by $B_{\mathrm{rel,PR}} = 1-f_{\mathrm{reabs,bb}}$ as a function of sample width and temperature, for a *planar* sample and one with idealized Lambertian surfaces (*diffuse*).

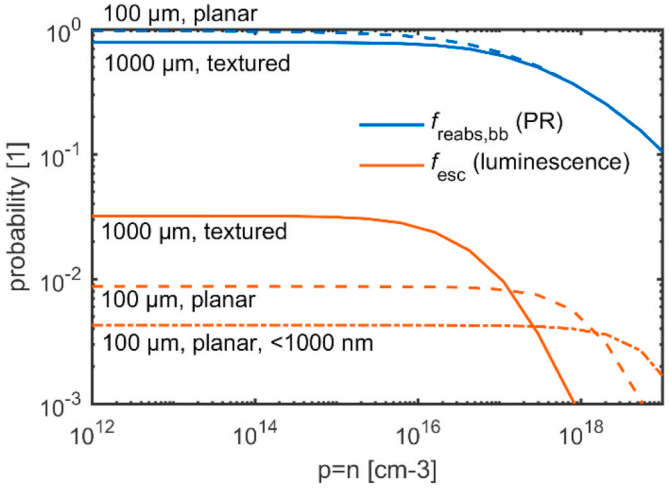

Fig. 7. c-dependence of band-to-band reabsorption and escape probability via FCA calculated by this work's model for two extreme cases: a 100 µm thick *planar* sample and a 1000 µm thick double-side wafer with Lambertian surfaces (*textured*). For the escape probability of the planar sample, a second curve is shown via integrating Equation (20) only up to 1000 nm, indicating the effect of a typical short-pass filter to reduce the influence of FCA.

calculated:

$$f_{esc} = \frac{\int \int_o^W f_{esc}(\lambda, z) dz \, r_{spont}(\lambda) d\lambda}{\int r_{spont}(\lambda) d\lambda} \quad (20)$$

With the non-degeneracy assumption, the exponent of the Fermi-level split of the spontaneous emission rate cancels in equations (19) and (20), thus the escape and reabsorption probabilities can be calculated via the spontaneous emission rate in thermal equilibrium and usually only once per unique set of optical sample properties and temperature. An exception is the case where FCA of injected carriers is significant, where equations (19) and (20) need to be calculated for each charge carrier density, see section 4.3 for a quantification of this effect.

As was shown in Ref. [25], the optical model used here can well be calibrated by a fit to a sample's measured RAT data, in particular when employing the simplification of a single internal reflection per side: R_{f1}=R_{fn} = R_f and R_{b1}=R_{bn} = R_b. This enables to quantitatively account for the amount of PR within an experimental sample with at least one scattering surface by i) measuring RAT (reflectance only is sufficient), ii) fitting the optical model in its simplified form, and iii) calculate $B_{rel,PR}$ by equations (5) and (17).

For the case of a double-side specular sample however, i.e. a planar sample, light-trapping and small-angle escape on the one hand, and reabsorption on the other hand, cannot be modelled with a unique set of internal reflections due to the different relevant angular distributions. This means that f_{reabs} cannot be determined by a calibration of the model to RAT measurements, but needs to be calculated by equation (18) including the Fresnel equations requiring knowledge of the surface coating's optical properties. Notably, due to reabsorption being dominated by total reflection in the planar case, the bare silicon results in Fig. 6 may be a reasonable approximation for a wide range of typical planar samples with non-absorbing and optically thin surface coatings due to having the same critical angle.

To give an impression of the magnitude of the PR effect, in Fig. 6 $B_{rel,PR}$ of a bare silicon sample is shown as a function of width and temperature for the planar and diffuse case described above. It can be seen that PR is a strong effect for typical lifetime samples, in particular for planar samples, and must therefore not be neglected when modeling absolute radiative recombination rates. Another finding is that for diffuse, i.e. textured samples, PR strongly depends on the width. This is important to consider e.g. in bulk lifetime determination based on the thickness variation method, for which the bulk lifetime is typically assumed independent of the width.

4.3. Influence of FCA on photon reabsorption

In the following, the influence of FCA on the PR effect, as well as on luminescence intensity is estimated by using this work's model. For this, the c-dependence of $f_{reabs,bb}$ and f_{esc} is modelled using α_{bb} of Schinke et al. [12], and α_{FCA} of Baker-Finch et al. [24] for a 1000 µm textured and a 100 µm planar sample. For calculating f_{esc} the internal reflections are set to their Lambertian limit of $1 - \frac{1}{n^2}$ for the textured sample, but to the perpendicular value of $\left(\frac{n-1}{n+1}\right)^2$ for the planar sample. $f_{reabs,bb}$ for the two cases is calculated as described in section 4.2. A perfect external transmission of $T_{ext} = 100\%$ was assumed along with a unity acceptance angle of $\Omega = 1$ *rad* for f_{esc}. Notably, a measured luminescence signal will also be influenced by the spectral efficiency of the measurement setup as the reabsorption is strongly wavelength dependent. Equation (20) then needs to additionally include the spectral sensitivity to determine the detection probability.

The results in Fig. 7 reveal the following observations:

i) For relatively thick samples (>several hundred µm), FCA has an influence on the escape probability at charge carrier densities as low as 10^{16} cm^{-3}. That means that the strict proportionality between radiative recombination and luminescence signal, which is fundamental to all popular luminescence based characterization techniques, becomes inaccurate. If a measurement is analyzed under such conditions, a correction e.g. by using this work's model should then be considered. The critical carrier density however becomes substantially higher when using a short-pass filter for detection, as the higher wavelengths most affected by FCA are then excluded.
ii) The onset for a significant c-dependence for PR is only for carrier densities around 10^{17} cm^{-3}, which is considered a minor effect for most silicon PV applications as for such carrier densities Auger recombination strongly dominates over radiative recombination.
iii) For typical doping levels of silicon wafers in PV ($\lesssim 10^{16}$cm^{-3}), FCA of charge carriers introduced by doping does not influence PR nor luminescence.

4.4. Modeling photon recycling for the interpretation of effective lifetime measurements

Finally, it is shown that the PR effect becomes observable in an effective lifetime measurement for the case of very-high-lifetime samples. The experimental details of the investigated sample reaching a lifetime of ~1/3 of a second are given in Ref. [26]. The reabsorption probability of this planar sample is calculated using this work's model for the sample width of 385 µm as a function of excess carrier density $\Delta n \approx n = p$. The effective lifetime curve is fitted with and without PR, using the latest Auger [27] and radiative recombination models, and having a background SRH defect lifetime and the surface recombination parameter J_0 as free variables.

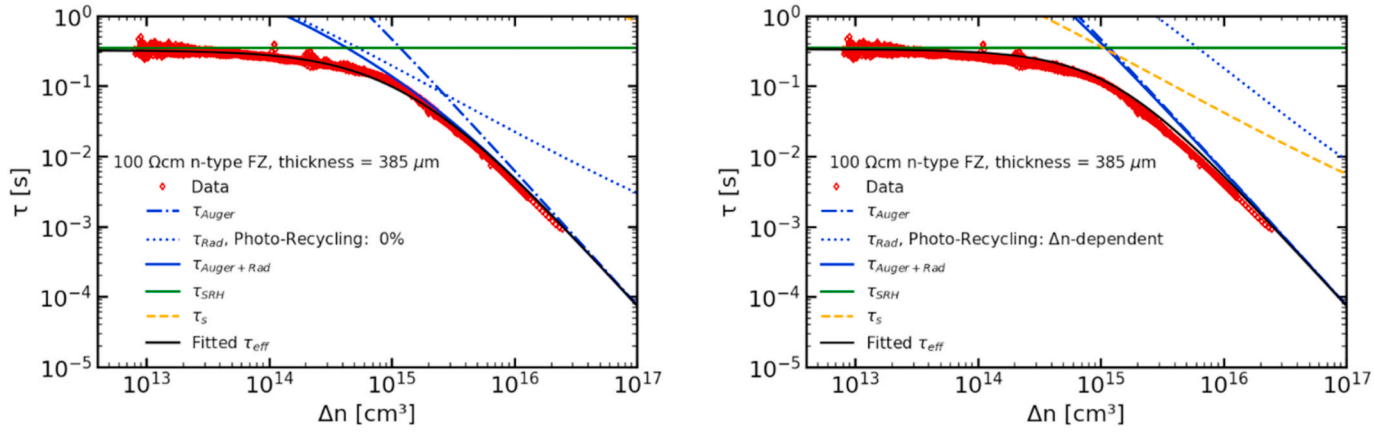

Fig. 8. Best fit of lifetime measurement without (*left*) and with (*right*) consideration of the PR effect via this work's model.

When not considering PR, see Fig. 8, left, the effective lifetime curve can only be reasonably fitted by assuming zero surface recombination. Still, around a charge carrier density of 10^{15} cm^{-3}, which is precisely the narrow window where radiative recombination is significant compared to both, SRH and Auger recombination, the measured lifetime slightly exceeds the modelled one. This hints to an overestimation of radiative recombination. With consideration of PR in Fig. 8, right, the fit results in a J_0 of 0.8 fA/cm^2 and an improved match of the curve's shape around 10^{15} cm^{-3}. Furthermore, a significant deviation becomes visible for high charge carrier densities. This is likely related to an overestimation of Auger recombination in Ref. [27], with one possible cause being the neglection of PR.

While the effect may seem only academic on first sight, the importance of considering PR might increase with ever increasing material and surface passivation quality, e.g. when quantifying very low surface recombination. A particular relevance is given already now in the ongoing work to improve the quantification of Auger recombination in silicon [27–29], for which this work's model will be used for consideration of PR.

5. Conclusions

This work reassesses the existing literature on quantitative modeling of radiative recombination in silicon for PV applications. It is found that the temperature-dependent fundamental radiative recombination coefficient, best quantified as $B_{\mathrm{rad,low}} n_{\mathrm{i},0}^2$, is known with satisfactory accuracy of ~10% by comparing values derived from most recent publications. The effects introducing a c-dependence of B_{rad}, quantified by the c-dependent scaling factor B_{rel}, are theoretically factored into an optical part, which is mainly the change of band-to-band absorption coefficient, and an electrical part, which is due to the change of $n_{\mathrm{i,eff}}$ via BGN. By comparing calculations of the electrical c-dependence using the BGN model of Schenk, with experimental data and the semi-empirical B_{rel} model of Altermatt et al., it is revealed that B_{rel} is fully dominated by the electrical BGN effect. This clarifies that Altermatt's B_{rel} model is in fact a quantification of BGN, and thus should not be mixed with the usage of Schenk's model for the sake of consistency. It might however be a useful alternative to Schenk's BGN model, by being mathematically much simpler, and by including temperature dependence in contrast to other simple BGN models. The finding also supports an assumption implicitly applied to all silicon solar cell modeling to date: the c-dependence of the band-to-band absorption coefficient is negligible for PV conditions.

Furthermore, this work introduces an extended analytical light-trapping model to quantify the effect of photon recycling, as well as the c-dependence of PR and luminescence signal introduced by FCA. The model routinely calculates escape reflection and transmission, which allows calibrating the model's inputs to such measurement data of experimental samples for the case of textured samples. For the case of planar samples, the effect of photon recycling is instead quantified theoretically. On an exemplary very-high-lifetime sample for which radiative recombination is observable in the effective lifetime, it is showcased that the inclusion of PR via this work's model significantly improves the theoretical fit of the effective lifetime curve. The model thus is useful when accurately analyzing very high lifetime measurements, e.g. for the extraction of very low surface recombination, or for an improved quantification of Auger recombination.

Finally, the model is used to predict the c-dependence of PR and of the luminescence signal introduced by FCA. It is shown that PR is largely independent from carrier density, as it becomes significant only at high charge carrier densities where Auger strongly dominates over radiative recombination. For the luminescence signal, FCA becomes significant for relatively thick wafers and charge carrier densities $> 10^{16}$ cm^{-3}, which then invalidates the direct proportionality between radiative recombination and luminescence signal, a fundamental assumption in most luminescence-based characterization techniques. When measuring under such non-typical conditions, the influence of FCA on the proportionality must therefore be considered, e.g. via a correction using this work's model.

CRediT authorship contribution statement

Andreas Fell: Conceptualization, Methodology, Software, Writing – original draft. **Tim Niewelt:** Conceptualization, Project administration, Funding acquisition, Investigation, Writing – review & editing. **Bernd Steinhauser:** Conceptualization, Investigation, Writing – review & editing. **Friedemann D. Heinz:** Conceptualization, Writing – review & editing. **Martin C. Schubert:** Supervision, Project administration, Funding acquisition, Writing – review & editing. **Stefan W. Glunz:** Supervision, Writing – review & editing.

Declaration of competing interest

The authors declare that they have no known competing financial interests or personal relationships that could have appeared to influence the work reported in this paper.

Acknowledgements

The authors would like to thank Pietro Altermatt for fruitful discussions and for sharing the experimental data, and Jonas Schön for fruitful discussions.

This work was supported in part by the German Federal Ministry for Economic Affairs and Energy (BMWi) and by the Industry Partners under Grant 0324204A and Grant 0324204C.

References

[1] W. Gerlach, H. Schlangenotto, H. Maeder, On the radiative recombination rate in silicon, Phys. Status Solidi (A) 13 (1) (1972) 277–283.
[2] E.H. Kennard, On the thermodynamics of fluorescence, Phys. Rev. 11 (1) (1918) 29–38.
[3] R.T. Ross, Some thermodynamics of photochemical systems, J. Chem. Phys. 46 (12) (1967) 4590–4593.
[4] P. Würfel, S. Finkbeiner, E. Daub, Generalized Planck's radiation law for luminescence via indirect transitions, Appl. Phys. A 60 (1) (1995) 67–70.
[5] T. Trupke, M.A. Green, P. Würfel, P.P. Altermatt, A. Wang, J. Zhao, R. Corkish, Temperature dependence of the radiative recombination coefficient of intrinsic crystalline silicon, J. Appl. Phys. 94 (8) (2003) 4930–4937.
[6] H. Schlangenotto, H. Maeder, W. Gerlach, Temperature dependence of the radiative recombination coefficient in silicon, Phys. Status Solidi (A) 21 (1) (1974) 357–367.
[7] H.T. Nguyen, S.C. Baker-Finch, D. Macdonald, Temperature dependence of the radiative recombination coefficient in crystalline silicon from spectral photoluminescence, Appl. Phys. Lett. 104 (11) (2014) 112105.
[8] P.P. Altermatt, F. Geelhaar, T. Trupke, X. Dai, A. Neisser, E. Daub, Injection dependence of spontaneous radiative recombination in crystalline silicon: experimental verification and theoretical analysis, Appl. Phys. Lett. 88 (26) (2006) 261901.
[9] D.K. Schroder, R.N. Thomas, J.C. Swartz, Free carrier absorption in silicon, IEEE J. Solid State Circ. 13 (1) (1978) 180–187.
[10] M.P. Lumb, M.A. Steiner, J.F. Geisz, R.J. Walters, Incorporating photon recycling into the analytical drift-diffusion model of high efficiency solar cells, J. Appl. Phys. 116 (19) (2014) 194504.
[11] A. Richter, M. Hermle, S.W. Glunz, Reassessment of the limiting efficiency for crystalline silicon solar cells, IEEE J. Photovoltaics 3 (4) (2013) 1184–1191.
[12] C. Schinke, P. Christian Peest, J. Schmidt, R. Brendel, K. Bothe, M.R. Vogt, I. Kröger, S. Winter, A. Schirmacher, S. Lim, H.T. Nguyen, D. Macdonald, Uncertainty analysis for the coefficient of band-to-band absorption of crystalline silicon, AIP Adv. 5 (6) (2015) 67168.

[13] R. Couderc, M. Amara, M. Lemiti, Reassessment of the intrinsic carrier density temperature dependence in crystalline silicon, J. Appl. Phys. 115 (9) (2014) 93705.
[14] P.P. Altermatt, A. Schenk, F. Geelhaar, G. Heiser, Reassessment of the intrinsic carrier density in crystalline silicon in view of band-gap narrowing, J. Appl. Phys. 93 (3) (2003) 1598–1604.
[15] R. Pässler, Dispersion-related description of temperature dependencies of band gaps in semiconductors, Phys. Rev. B 66 (8) (2002).
[16] A. Schenk, Finite-temperature full random-phase approximation model of band gap narrowing for silicon device simulation, J. Appl. Phys. 84 (7) (1998) 3684–3695.
[17] E. Daub, P. Wurfel, Ultra-low values of the absorption coefficient for band-band transitions in moderately doped Si obtained from luminescence, J. Appl. Phys. 80 (9) (1996) 5325–5331.
[18] Di Yan, A. Cuevas, Empirical determination of the energy band gap narrowing in highly doped n+ silicon, J. Appl. Phys. 114 (4) (2013) 44508.
[19] Di Yan, A. Cuevas, Empirical determination of the energy band gap narrowing in p + silicon heavily doped with boron, J. Appl. Phys. 116 (19) (2014) 194505.
[20] P.A. Basore, Numerical modeling of textured silicon solar cells using PC-1D, IEEE Trans. Electron. Dev. 37 (2) (1990) 337–343.
[21] C. Schinke, D. Hinken, J. Schmidt, K. Bothe, R. Brendel, Modeling the spectral luminescence emission of silicon solar cells and wafers, IEEE J. Photovoltaics 3 (3) (2013) 1038–1052.
[22] M.A. Green, Lambertian light trapping in textured solar cells and light-emitting diodes: analytical solutions, Prog. Photovoltaics Res. Appl. 10 (4) (2002) 235–241.
[23] M.J. Kerr, A. Cuevas, P. Campbell, Limiting efficiency of crystalline silicon solar cells due to Coulomb-enhanced Auger recombination, Prog. Photovoltaics Res. Appl. 11 (2) (2003) 97–104.
[24] S.C. Baker-Finch, K.R. McIntosh, Di Yan, K.C. Fong, T.C. Kho, Near-infrared free carrier absorption in heavily doped silicon, J. Appl. Phys. 116 (6) (2014).
[25] A. Fell, W. Wirtz, H. Höffler, J. Greulich, Determining the generation rate of silicon solar cells from reflection and transmission measurements by fitting an analytical optical model, in: 2019 IEEE 46th Photovoltaic Specialists Conference (PVSC), Chicago, IL, USA, IEEE, Piscataway, NJ, 2019, pp. 3037–3041.
[26] B. Steinhauser, J.-I. Polzin, F. Feldmann, M. Hermle, S.W. Glunz, Excellent surface passivation quality on crystalline silicon using industrial-scale direct-plasma TOPCon deposition technology, Solar RRL 2 (7) (2018) 1800068.
[27] A. Richter, S.W. Glunz, F. Werner, J. Schmidt, A. Cuevas, Improved quantitative description of Auger recombination in crystalline silicon, Phys. Rev. B 86 (16) (2012) 165202.
[28] T. Niewelt, A. Richter, T.C. Kho, N.E. Grant, R.S. Bonilla, B. Steinhauser, J.-I. Polzin, F. Feldmann, M. Hermle, J.D. Murphy, S.P. Phang, W. Kwapil, M. C. Schubert, Taking monocrystalline silicon to the ultimate lifetime limit, Sol. Energy Mater. Sol. Cell. 185 (2018) 252–259.
[29] B.A. Veith-Wolf, S. Schäfer, R. Brendel, J. Schmidt, Reassessment of intrinsic lifetime limit in n-type crystalline silicon and implication on maximum solar cell efficiency, Sol. Energy Mater. Sol. Cell. 186 (2018) 194–199.